

LAMPIRAN



Voltage Transducer LV 25-P

For the electronic measurement of currents: DC, AC, pulsed..., with galvanic separation between the primary circuit and the secondary circuit.

$$I_{PN} = 10 \text{ mA}$$

$$V_{PN} = 10 \dots 500 \text{ V}$$



Electrical data

| | | | |
|-----------|----------------------------------|---------------------------------------|----------------------|
| I_{PN} | Primary nominal rms current | 10 | mA |
| I_{PM} | Primary current, measuring range | 0 ... ± 14 | mA |
| R_{in} | Measuring resistance | $R_{in} \dots R_{in, max}$ | |
| | with $\pm 12 \text{ V}$ | $\pm 10 \text{ mA}$ | 30 ... 190 Ω |
| | | $\pm 14 \text{ mA}$ | 30 ... 100 Ω |
| | with $\pm 15 \text{ V}$ | $\pm 10 \text{ mA}$ | 100 ... 350 Ω |
| | | $\pm 14 \text{ mA}$ | 100 ... 150 Ω |
| I_{out} | Secondary nominal rms current | 25 | mA |
| K_n | Conversion ratio | 2500 : 1000 | |
| U_c | Supply voltage ($\pm 5\%$) | $\pm 12 \dots 15$ | V |
| I_c | Current consumption | 10 ($\pm 15 \text{ V}$) + I_{out} | mA |

Accuracy - Dynamic performance data

| | | | |
|--------------|--|---|------------------------|
| X_d | Overall accuracy @ I_{PM} , $T_A = 25^\circ\text{C}$ | ± 0.9 | % |
| | | ± 0.8 | % |
| ϵ_L | Linearity error | < 0.2 | % |
| | | Typ | Max |
| I_o | Offset current @ $I_{PM} = 0$, $T_A = 25^\circ\text{C}$ | ± 0.15 | mA |
| I_{OT} | Temperature variation of I_o | $0^\circ\text{C} \dots +25^\circ\text{C}$ | $\pm 0.06 \pm 0.25$ mA |
| | | $+25^\circ\text{C} \dots +70^\circ\text{C}$ | $\pm 0.10 \pm 0.35$ mA |
| t_r | Step response time ¹⁾ to 90% of I_{PM} | 40 | μs |

General data

| | | | |
|-------|--|------------------------------|------------------|
| T_A | Ambient operating temperature | 0 ... +70 | $^\circ\text{C}$ |
| T_S | Ambient storage temperature | -25 ... +85 | $^\circ\text{C}$ |
| R_p | Resistance of primary winding @ $T_A = 70^\circ\text{C}$ | 250 | Ω |
| R_s | Resistance of secondary winding @ $T_A = 70^\circ\text{C}$ | 110 | Ω |
| m | Mass | 22 | g |
| | Standards | EN 50178:1997 UL 508:2010 | |

Features

- Closed loop (compensated) current transducer using the Hall effect
- Insulating plastic case recognized according to UL 94-V0.

Principle of use

- For voltage measurements, a current proportional to the measured voltage must be passed through an external resistor R_i which is selected by the user and installed in series with the primary circuit of the transducer.

Advantages

- Excellent accuracy
- Very good linearity
- Low thermal drift
- Low response time
- High bandwidth
- High immunity to external interference
- Low disturbance in common mode.

Applications

- AC variable speed drives and servo motor drives
- Static converters for DC motor drives
- Battery supplied applications
- Uninterruptible Power Supplies (UPS)
- Power supplies for welding applications.

Application domain

- Industrial.

Note: ¹⁾ $R_i = 25 \text{ k}\Omega$ (L/R constant, produced by the resistance and inductance of the primary circuit).

TLP250

Transistor Inverter

Inverter For Air Conditioner

IGBT Gate Drive

Power MOS FET Gate Drive

The TOSHIBA TLP250 consists of a GaAlAs light emitting diode and a integrated photodetector.

This unit is 8-lead DIP package.

TLP250 is suitable for gate driving circuit of IGBT or power MOS FET.

- Input threshold current: $I_F = 5\text{mA (max.)}$
- Supply current (I_{CC}): 11mA (max.)
- Supply voltage (V_{CC}): $10\text{--}35\text{V}$
- Output current (I_O): $\pm 1.5\text{A (max.)}$
- Switching time (t_{PLH}/t_{PHL}): $0.5\mu\text{s (max.)}$
- Isolation voltage: $2500\text{V}_{rms}(\text{min.})$
- UL recognized: UL1577, file No.E67349
- Option(D4)

VDE Approved : DIN EN60747-5-2

Maximum Operating Insulation Voltage : 800V_{PK}

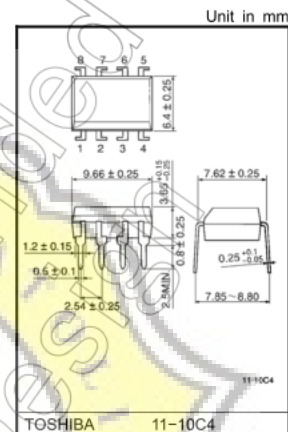
Highest Permissible Over Voltage : 4000V_{PK}

(Note)-When a EN60747-5-2 approved type is needed,

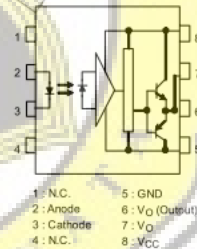
Please designate "Option(D4)"

Truth Table

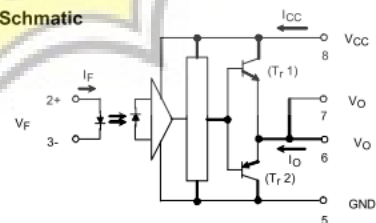
| | | T_{r1} | T_{r2} |
|-----------|-----|----------|----------|
| Input LED | On | On | Off |
| | Off | Off | On |



Pin Configuration (top view)



Schematic



A 0.1 μF bypass capacitor must be connected between pin 8 and 5 (See Note 5).



dsPIC30F4011/4012

dsPIC30F4011/4012 Enhanced Flash 16-bit Digital Signal Controller

Note: This data sheet summarizes features of this group of dsPIC30F devices and is not intended to be a complete reference source. For more information on the CPU, peripherals, register descriptions and general device functionality, refer to the *dsPIC30F Family Reference Manual* (DS70046). For more information on the device instruction set and programming, refer to the *dsPIC30F Programmer's Reference Manual* (DS70030).

High Performance Modified RISC CPU:

- Modified Harvard architecture
- C compiler optimized instruction set architecture with flexible addressing modes
- 84 base instructions
- 24-bit wide instructions, 16-bit wide data path
- 48 Kbytes on-chip Flash program space (16K instruction words)
- 2 Kbytes of on-chip data RAM
- 1 Kbytes of non-volatile data EEPROM
- Up to 30 MIPS operation:
 - DC to 40 MHz external clock input
 - 4 MHz-10 MHz oscillator input with PLL active (4x, 8x, 16x)
- 30 interrupt sources
 - 3 external interrupt sources
 - 8 user selectable priority levels for each interrupt source
 - 4 processor trap sources
- 16 x 16-bit working register array

DSP Engine Features:

- Dual data fetch
- Accumulator write back for DSP operations
- Modulo and Bit-Reversed Addressing modes
- Two, 40-bit wide accumulators with optional saturation logic
- 17-bit x 17-bit single cycle hardware fractional/integer multiplier
- All DSP instructions single cycle
- \pm 16-bit single cycle shift

Peripheral Features:

- High current sink/source I/O pins: 25 mA/25 mA
- Timer module with programmable prescaler:
 - Five 16-bit timers/counters; optionally pair 16-bit timers into 32-bit timer modules
- 16-bit Capture input functions
- 16-bit Compare/PWM output functions
- 3-wire SPI™ modules (supports 4 Frame modes)
- I²C™ module supports Multi-Master/Slave mode and 7-bit/10-bit addressing
- 2 UART modules with FIFO Buffers
- 1 CAN modules, 2.0B compliant

Motor Control PWM Module Features:

- 6 PWM output channels
 - Complementary or Independent Output modes
 - Edge and Center Aligned modes
- 3 duty cycle generators
- Dedicated time base
- Programmable output polarity
- Dead-time control for Complementary mode
- Manual output control
- Trigger for A/D conversions

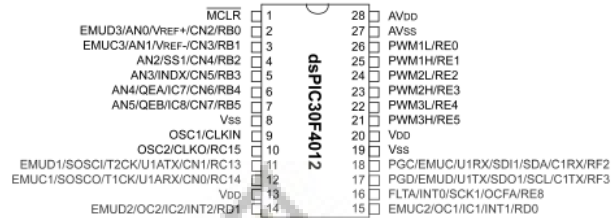
Quadrature Encoder Interface Module Features:

- Phase A, Phase B and Index Pulse input
- 16-bit up/down position counter
- Count direction status
- Position Measurement (x2 and x4) mode
- Programmable digital noise filters on inputs
- Alternate 16-bit Timer/Counter mode
- Interrupt on position counter rollover/underflow

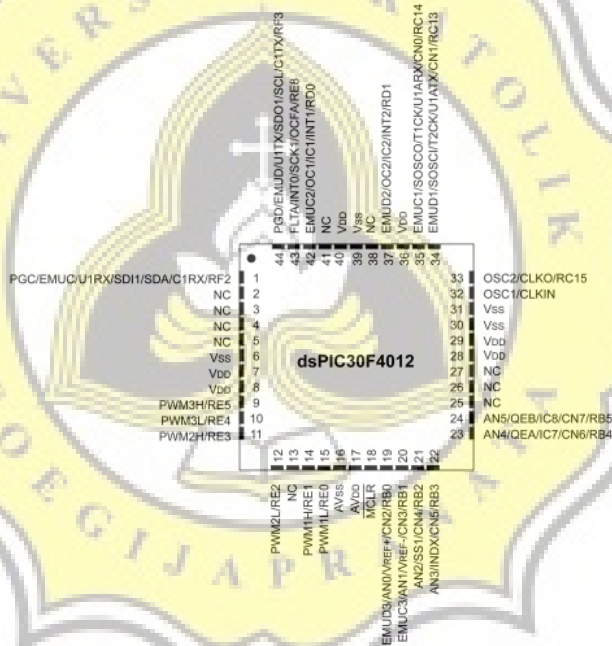
dsPIC30F4011/4012

Pin Diagrams (Continued)

28-Pin SPDIP 28-Pin SOIC

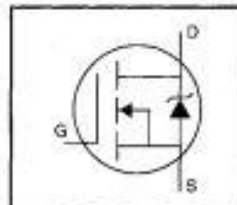


44-Pin QFN



HEXFET® Power MOSFET

- Dynamic dv/dt Rating
- Repetitive Avalanche Rated
- Isolated Central Mounting Hole
- Fast Switching
- Ease of Paralleling
- Simple Drive Requirements



$$V_{DSS} = 500V$$

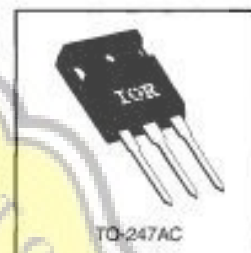
$$R_{DS(on)} = 0.27\Omega$$

$$I_D = 20A$$

Description

Third Generation HEXFETs from International Rectifier provide the designer with the best combination of fast switching, ruggedized device design, low on-resistance and cost-effectiveness.

The TO-247 package is preferred for commercial-industrial applications where higher power levels preclude the use of TO-220 devices. The TO-247 is similar but superior to the earlier TO-218 package because of its isolated mounting hole. It also provides greater creepage distance between pins to meet the requirements of most safety specifications.



TO-247AC

DATA
SHEETS

Absolute Maximum Ratings

| | Parameter | Max. | Units |
|---------------------------|--|-----------------------|---------------|
| $I_D @ T_C = 25^\circ C$ | Continuous Drain Current, $V_{GS} @ 10V$ | 20 | A |
| $I_D @ T_C = 100^\circ C$ | Continuous Drain Current, $V_{GS} @ 10V$ | 13 | |
| I_{DM} | Pulsed Drain Current ϕ | 80 | |
| $P_D @ T_C = 25^\circ C$ | Power Dissipation | 280 | W |
| | Linear Derating Factor | 2.2 | W/ $^\circ C$ |
| V_{GS} | Gate-to-Source Voltage | ± 20 | V |
| E_{AS} | Single Pulse Avalanche Energy ϕ | 960 | mJ |
| I_{AR} | Avalanche Current ϕ | 20 | A |
| E_{AR} | Repetitive Avalanche Energy ϕ | 28 | mJ |
| dv/dt | Peak Diode Recovery dv/dt ϕ | 3.5 | V/ns |
| T_J | Operating Junction and | -55 to $+180$ | $^\circ C$ |
| T_{STG} | Storage Temperature Range | | |
| | Soldering Temperature, for 10 seconds | 300 (1.8mm from case) | |
| | Mounting Torque, 6-32 or M3 screw | 10 lbf-in (1.1 N-m) | |

Thermal Resistance

| | Parameter | Min. | Typ. | Max. | Units |
|-----------------|-------------------------------------|------|------|------|--------------|
| $R_{\theta JC}$ | Junction-to-Case | — | — | 0.45 | $^\circ C/W$ |
| $R_{\theta CS}$ | Case-to-Sink, Flat, Greased Surface | — | 0.24 | — | |
| $R_{\theta JA}$ | Junction-to-Ambient | — | — | 40 | |

DC/DC Converter B_S-1WR2 & B_D-1WR2 series

MORNSUN®

1W, Fixed input voltage, isolated & unregulated single output



FEATURES

- Continuous short-circuit protection
- Operating temperature range: -40°C to +105°C
- Conversion efficiency high up to 80%
- Miniature SIP/DIP package, International standard pin-out
- Isolation voltage: 1.5K VDC
- EN60950, UL60950 Approval

UL US CE Patent Protection RoHS



B_S-1WR2 & B_D-1WR2 series are specially designed for applications where an isolated voltage is required in a distributed power supply system. They are suitable for:

1. Where the voltage of the input power supply is stable (voltage variation: $\pm 10\%$);
2. Where isolation between input and output is necessary (isolation voltage: $\geq 1500\text{VDC}$);
3. Where the output voltage regulation and the ripple & noise of the output voltage is not strictly required;
4. Typical applications: digital circuit condition; normal low-frequency artificial circuit condition; relay drive circuit and data switching circuit condition, etc.

| Selection Guide | | | | | | |
|-----------------|-------------|---------------------|----------------------|--------------------------------|---------------------------------------|--------------------------|
| Certification | Part No. | Input Voltage (VDC) | | Output | | Max. Capacitive Load(μF) |
| | | Nominal (Range) | Output Voltage (VDC) | Output Current (mA)(Max./Min.) | Efficiency (%)(Min./Typ.) @ Full Load | |
| UL/CE | B0003S-1WR2 | 3.3 (2.97-3.63) | 3.3 | 303/30 | 68/72 | 220 |
| | B0005S-1WR2 | | 5 | 200/20 | 75/78 | |
| | B0012S-1WR2 | | 12 | 84/9 | 75/80 | |
| | B0030S-1WR2 | | 3.3 | 303/30 | 68/72 | |
| UL/CE | B0030D-1WR2 | 5 (4.5-5.5) | 5 | 200/20 | 72/76 | |
| | B0003S-1WR2 | | 3.3 | 303/30 | 68/72 | |
| | B0005S-1WR2 | | 5 | 200/20 | 75/80 | |
| | B0009S-1WR2 | | 9 | 111/12 | 75/80 | |
| UL/CE | B0012S-1WR2 | 12 (10.5-13.2) | 12 | 84/9 | 75/80 | |
| | B0015S-1WR2 | | 15 | 67/7 | 75/80 | |
| | B0024S-1WR2 | | 24 | 42/4 | 75/80 | |
| | B0030D-1WR2 | | 3.3 | 303/30 | 68/72 | |
| UL/CE | B0030S-1WR2 | 12 (10.5-13.2) | 5 | 200/20 | 76/80 | |
| | B0009S-1WR2 | | 9 | 111/12 | 75/80 | |
| | B0012D-1WR2 | | 12 | 84/9 | 75/80 | |
| | B0015D-1WR2 | | 15 | 67/7 | 75/80 | |
| UL/CE | B0024D-1WR2 | 12 (10.5-13.2) | 24 | 42/4 | 75/80 | |
| | B1203S-1WR2 | | 3.3 | 303/30 | 68/72 | |
| | B1205S-1WR2 | | 5 | 200/20 | 75/80 | |
| | B1209S-1WR2 | | 9 | 111/12 | 75/80 | |
| UL/CE | B1212S-1WR2 | 12 (10.5-13.2) | 12 | 84/9 | 75/80 | |
| | B1215S-1WR2 | | 15 | 67/7 | 75/80 | |
| | B1224S-1WR2 | | 24 | 42/4 | 75/80 | |
| | B1203D-1WR2 | | 3.3 | 303/30 | 68/72 | |
| UL/CE | B1205D-1WR2 | 12 (10.5-13.2) | 5 | 200/20 | 75/80 | |
| | B1209D-1WR2 | | 9 | 111/12 | 75/80 | |
| | B1212D-1WR2 | | 12 | 84/9 | 75/80 | |
| | B1215D-1WR2 | | 15 | 67/7 | 75/80 | |

MORNSUN®

MORNSUN GUANGZHOU SCIENCE & TECHNOLOGY CO., LTD.

2015.09.21-A/4

Page 1 of 6

MORNSUN Guangzhou Science & Technology Co., Ltd. reserves the copyright and right of final interpretation

Doc vs Internet + Library

96.06% Originality

3.94% Similarity

89 Sources

Web sources: 52 sources found

| | |
|---|-------|
| 1. http://www.datasheet.hk/view_online.php?id=11453828&e=0070%5cm68hc05b32_591718.pdf | 0.37% |
| 2. https://docplayer.es/901467-P-a-g-i-n-a-1-penetration-testing-with-back-track.html | 0.22% |
| 3. http://chousensha.github.io/blog/2014/08/16/pentest-lab-webgoat/ | 0.22% |
| 4. https://michael-myers.github.io/blog/ | 0.22% |
| 5. https://piki.elektrodz.pl/45582,11a8td.html | 0.22% |
| 6. https://wikimonde.com/article/Sigles_de_deux_lettres_suivies_d%27un_chiffre | 0.22% |
| 7. https://www.microchip.com/mymicrochip/filehandler.aspx?ddocname=en023872 | 0.2% |
| 8. https://www.microchip.com/mymicrochip/filehandler.aspx?ddocname=en019507 | 0.2% |
| 9. https://www.ida.mil/Portals/104/Documents/DLMS/Library/JumpStart/JumpStartPMP3.1.doc | 0.19% |
| 10. https://www.lepetitjournal.be/normie_sortie.aspx | 0.19% |
| 11. https://docplayer.es/56343295-Diseno-de-un-modelo-de-evaluacion-de-entornos-virtuales-de-ense | 0.19% |
| 12. https://docplayer.fr/70596306-Mission-d-apui-au-departement-de-mayotte-sur-le-pilotage-de-la-pr | 0.19% |
| 13. http://davidstoday.org/en/document/book/show/v | 0.19% |
| 14. https://www.chapters.indigo.ca/fr-ca/livres/embodiment-logic-giveness-to-theological-analysis/9780802... | 0.17% |
| 15. https://www.chapters.indigo.ca/fr-ca/livres/when-the-emperor-was-divine/9780385721813-article.h... | 0.17% |
| 16. https://www.studymode.com/topic/Computer-network | 0.17% |
| 17. https://www.planet-cards.com/texte-sah/versaire | 0.17% |
| 18. https://www.ncbi.nlm.nih.gov/pmc/articles/PMC4732070/ | 0.15% |
| 19. https://www.mdpi.com/2079-9439/6/3/67/html | 0.15% |
| 20. https://codegolf.meta.stackexchange.com/questions/2140/sandbox-for-proposed-challenges/8248 | 0.15% |
| 21. http://www.mdpi.com/1422-0067/12/12/3750/html | 0.15% |
| 22. http://europepmc.org/articles/PMC3673407 | 0.15% |
| 23. https://www.orcad.com/documentation/pspice-advanced-analysis-user-guide | 0.15% |
| 24. https://www.math.union.edu/~category/number-theory/ | 0.15% |
| 25. https://studres.net/preview/608053-page-15 | 0.15% |
| 26. http://www.utdallas.edu/~zhoud/EE%203130/2019_tutorial_Spartan3_home_PO.pdf | 0.15% |
| 27. https://edberry.com/blog/climate-physics/how-hypothesis/human-co2-not-change-climate | 0.15% |
| 28. https://www.microchip.com/mymicrochip/filehandler.aspx?ddocname=en011813 | 0.15% |
| 29. https://open.library.utoronto.ca/10062112 | 0.15% |
| 30. http://www.cplusplus.com/forum/general/27808 | 0.15% |
| 31. https://www.csis.gc.ca/uk/its/docs/SIGDA-Compendium-1994-2004/papers/1995/ccad95.pdf/files... | 0.15% |
| 32. https://www.scribd.com/document/3259788/12da80 | 0.15% |
| 33. https://b-ok.xyz/book/3259788/12da80 | 0.15% |
| 34. http://www.fh.sk/files/katedry/kove/predmety/Prognosticke_modely/Edrometric_Models.pdf | 0.15% |

Similarity
Similarity from a chosen source
Possible character replacement
Common
References




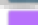
| | |
|---|-------|
| 35. https://www.eng.ox.ac.uk/~labejp/Seminar/Simulink/Simulink_Introduction.pdf | 0.15% |
| 36. https://StudFiles.net/preview/5083044/page:9 | 0.15% |
| 37. http://iisatech.com/murdocca/CAO/PracticeProblems.pdf | 0.15% |
| 38. http://www.cfm.brown.edu/people/dobrush/am33/SymPy/index.html | 0.15% |
| 39. http://ua-referat.com/%D0%9A%D0%BE%D1%80%D0%B5%D0%BB%D1%8F%D1%86%D1%9... | 0.15% |
| 40. https://www.tasc.tas.gov.au/students/courses/mathematics/mts415118 | 0.15% |
| 41. https://docplayer.info/45727151-Vol-iii-no-1-februari-2017-issn.html | 0.15% |
| 42. https://introcs.cs.princeton.edu/java/32class | 0.15% |
| 43. http://introcs.cs.princeton.edu/home/chapter1.pdf | 0.15% |
| 44. http://hildalarrondo.net/wp-content/uploads/2010/11/Capitulo-3-Extractor-de-Radar-.pdf | 0.15% |
| 45. http://elctromymagne.blogspot.com/2014 | 0.15% |
| 46. https://www.mdpi.com/1424-8220/8/4/2082/htm | 0.15% |
| 47. https://www.microchip.com/mymicrochip/filehandler.aspx?ddocname=en011653 | 0.15% |
| 48. http://elcodis.com/parts/1313825/MC68HC1621CFG35.html | 0.15% |
| 49. https://katie.mtech.edu/classes/archives15/csc156/Slides/10%20-%20Objects%20Variables%2... | 0.15% |
| 50. https://vdocuments.mx/coi_testing-manual-v6-feb-8.html | 0.15% |
| 51. https://ww1.microchip.com/downloads/en/devicedoc/39881e.pdf | 0.15% |
| 52. http://projectzimg.be/nl/dossier2/MBPoe1604W00_N_03/standveiligheid-bij-houten-gevelbekledin | 0.15% |

Web omitted sources: 1 source found

| | |
|--|-------|
| 1. http://repository.unika.ac.id/13436/5/12-50.0015%20F%20Dian%20Fajar%20Waluyon%20BAB%20... | 0.35% |
|--|-------|

Library sources: 24 sources found

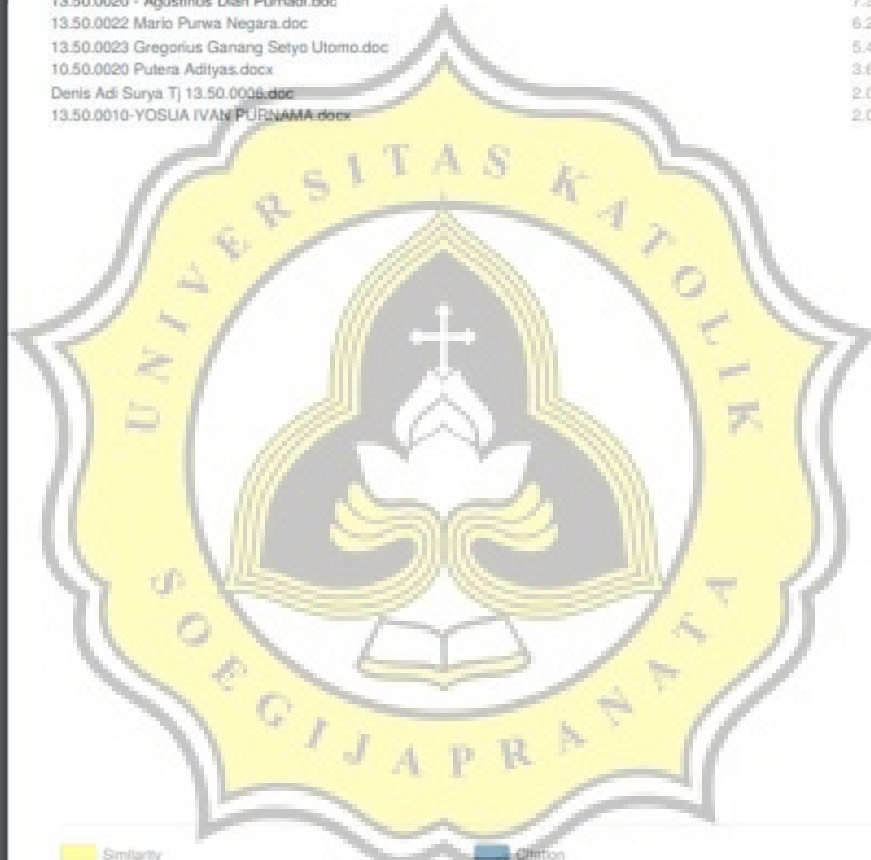
| | |
|--|-------|
| 13.50.0009 Naomi Intan H.docx | 2.21% |
| 13.50.0016 - STEFANUS KRISTIAN ANDREANTO.docx | 1.52% |
| 13.50.0004-ABRAM ALAM SUHARDI.docx | 0.54% |
| 14.F1.0010 Wira Adhitama.docx | 0.84% |
| 14.F1.0026 Natanael Novalutli.docx | 0.84% |
| 14.F1.0026 Natanael (revisi).docx | 0.56% |
| 15.F1.0018 - RUGRASENA (KP).docx | 0.35% |
| 15.F1.0018 Ugrasena revisi 3 .docx | 0.35% |
| monitoringAiatListik.pdf | 0.35% |
| 15.F1.0018 R.Ugrasena revisi 2 .docx | 0.35% |
| 16.H1.0018_Maria Sri.docx.docx | 0.32% |
| Christiana Nathalia 15.H1.0007 REVISI.docx | 0.15% |
| 16.H1.0043 AHMADI YOGI PRATAMA.docx.docx | 0.15% |
| 14.G1.0104Tjoa, Gracia Aline Suprapto (1).docx | 0.15% |
| Christiana Nathalia M 15.H1.0007.docx | 0.15% |
| Christiana Nathalia M 15.H1.0007 Rev 1.docx | 0.15% |
| Liem, Vito Reinaldo H-5 JUNI.docx | 0.15% |
| 16.H1.0043 AHMADI YOGI PRATAMA.docx | 0.15% |
| TEGAR STARRYSTIA 27 Maret.docx | 0.15% |
| 13.32.0004 - Liem, Vito Reinaldo- 8 MEI.docx | 0.15% |
| Tjoa, Gracia Aline Suprapto-AUDIT10 MEI.doc | 0.15% |
| 13.32.0004 - Liem, Vito Reinaldo H-4 JUNI.docx | 0.15% |

 Similarity
 Similarity from a chosen source
 Possible character replacement
 Citation
 References

MAHARANI LINTANG SIWI 27 Maret.docx 0.15%
14.G1.0104 TJQA GRACIA ALINE S.-7 DES.doc 0.15%

Library omitted sources: 12 sources found

13.50.0013 Hendra Winarto.doc 46.97%
KONVERTER C-DUMP TANPA INDUKTOR UNTUK PENGGERAK MOTOR SWITCH.doc 17.37%
13.50.0017 Sabar Santoso.docx 8.99%
13.50.0012 - Alvin Dharmawan Sugiarto II.doc 8.32%
13.50.0002-ardian haryanto.doc 8.1%
13.50.0012 - Alvin Dharmawan Sugiarto.doc 8.1%
13.50.0020 - Agustinus Dian Purnadi.doc 7.36%
13.50.0022 Mario Purwa Negara.doc 6.22%
13.50.0023 Gregorius Ganang Setyo Utomo.doc 5.42%
10.50.0020 Putera Adityas.docx 3.64%
Denis Adi Surya TJ 13.50.0006.doc 2.06%
13.50.0010-YOSUA IVAN PURNAMA.docx 2.06%



 Similarity
 Similarity from a chosen source
 Possible character replacement
 Citation
 References



SCORed 18



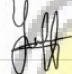
CERTIFICATE OF PARTICIPATION

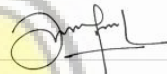
PRESENTED TO

KHO LUKAS BUDI SETIAWAN

FOR THE VALUABLE CONTRIBUTION AS
PRESENTER

AT 2018 IEEE STUDENT CONFERENCE AND ON RESEARCH AND DEVELOPMENT (SCORED)
AT BANGI GOLF RESORT, BANGI, MALAYSIA FROM THE 26TH TO THE 28TH OF NOVEMBER 2018


PROF. DR. MOHAMAD YUSOFF ALIAS
CONFERENCE CHAIR


ASSOC. PROF. DR. MOHAMMAD FAIZAL AHMED FAUZI
CONFERENCE GENERAL CHAIR

Analysis Performance of Capacitor Voltage in C-Dump Converter for SRM Drive

Kho Lukas Budi Setiawan, Slamet Riyadi
Department of Electrical Engineering
Soegijapranata Catholic University
Semarang, Indonesia
kho.lukas.b.s@gmail.com

Abstract— Switched reluctance motors have various converter topologies to control power, speed & operation. Conventional C-dump converter topologies will be discussed in this paper. Ease of control, simple construction, and low cost are the basis for choosing the type of converter. SRM is the best competitor for induction motors because the high torque ratio to Switched Reluctance Motors is more desirable than Induction Motors. This converter provides fast magnetization and rapid demagnetization of phase windings which prevents motor operation in generating mode. This avoids the formation of negative torque ripples. It also utilizes the energy stored in the winding phase & it can be a feedback to the source. Several new topology modifications from C-dump are able to utilize this stored energy to get out of the motor winding of the next stage.

Keywords—C-dump; energy recovery; capacitor; voltage control; speed; switch reluctance

I. INTRODUCTION

Nowadays the problematical of economic and environmental are considered the main reasons for the development of electric vehicles. Once of the major problem of pollution comes from burning fossil-fueled and the increasing number of vehicle riders. It also triggers a scarcity of fossil fuels. To overcome the problem, then the electric vehicles are developed. An electric vehicle used a conventional DC (Direct Current) motor because the torque was stronger to an AC (Alternating Current) motor. But conventional DC motor has a weakness that is on the brush. Along with the development of the era of electric vehicles using modern motors began to be applied.

The BLDC (Brush Less Direct Current) motor has great demand because it has great power, high efficiency, and low maintenance costs. But it also has some weaknesses in the rotor it is made from permanent magnets so the cost becomes more expensive [1]. From the weakness is then developed again electric vehicles using the type of motor switched reluctance. The main SRM (Switch Reluctance Motor) drive limitations are: (a) acoustic noise and torque ripple is present due to the structure of SRM, (b) along energy removal period is usually required due to extreme energy from the high winding inductance [2][3][8].

Now, for its basic operation SRM drive requires a power converter and control system. Modern power semiconductor

technology and high-speed controllers give the way for renewed interest in SRM drives [5]. The converter topologies C-dump converter to reduce the voltage drop and reduce the control circuitry complexity [6] [7]. It use to stores energy that come from the commutating phase into the dump capacitor, that can become a feedback for the source or can become utilized to excite the next phase stator winding. However, the attractions of SRM drives will be significantly enhanced if the machine can maximize the power and voltage control. This paper is an attempt to explore and prove the efficiency of conventional C-dump converter for this possibility.

II. RESEARCH METHODS

A. Switched Reluctance Motor

The inductance phase is operated when the stator pole excited by the energy, it produces magnetic field of north poles & south poles on each pole tip of the motor stator winding depending to the current direction that flow into the phase winding in stator.

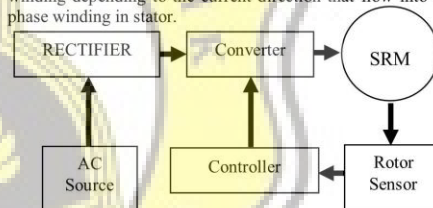


Fig.1. Switched Reluctance Motor Functional Block Diagram

SRM power torque production depends on the level of inductance phase change and the current phase change. The torque result is discrete and highly dependent on the position of the motor poles. The resulting torque formula is given by the following equation.[1]:

$$T = \frac{i^2}{2} \frac{dL(i, \theta)}{dt} \quad (1)$$

Where,

i = current in the phase winding

B. Conventional C-Dump

The converter is very important to provide DC (Direct Current) pulses to the each winding phase. The contributions of converters are greatly to the performance of drives in the system. For smoothest motor operations the design of the converter and work are very important, also to control the speed of the motor, reduce torque ripple at the output [2]. Each phase of the winding in stator must be able control by the converter independently. The low number of switch in the converter must be designed to provide the ability of fast magnetization & fast demagnetizing voltage to the each phase stator winding which is prevents the negative torque ripples.

The converter is consists of the semiconductor circuits & the power switches that provides DC (direct current) pulses to the winding of the stator. The type selection of the size, design of the converter & the numbers of buttons are depends on the selection of the topology. The converter topology is chosen based on the drive system application. Choosing the right converter topology is very important for reducing complexity, costs, and for better drive performance. The high switching frequencies affects the performance of motor speed, but also giving more the switching losses to the motor converter. The higher of samplings also offer a smaller lags of the system, and produce more stable system.

C. Operation Mode

In this converter, the energy that come from the phase winding is transfer into the dump capacitor before the energy reaches the aligned position. The voltage value of the capacitor in the system minimal set is twice of the value source voltage in order to apply fast demagnetization in stator of the motor. The energy from a capacitor transfer to the source using a chopper operating as a buck converter.

When phase L_1 is connected to the source, the winding becomes magnetized. The phase voltage are rises to the V_{DC} value and the current value is more than I_{max} , and then the diode D_1 is become forward biased because of the reversal of the polarity phase in L_1 and removes the energy stored in phase (Demagnetization Proses) to the exhaust the dump capacitor. The capacitor is stores this transfer energy and maintains the capacitor voltage above the V_{DC} source. In Q_4 switch it controls the voltage in the capacitor dump and the function of energy transfer to the source from the capacitor. Fig. 2, shows conventional C-dump of the converter, this consists of a dump capacitor & the chopper switch D_4 , L_C & Q_4 [3]. This transfers the stored energy into the capacitor that is discharged to the source.

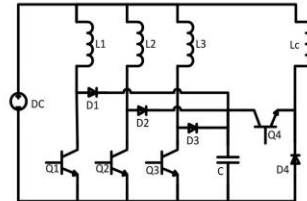


Fig. 2. Conventional C-Dump Converter

In this various of the converter operation mode of this conventional converter of C-dump are explained in the below :

In Fig. 3, switch Q_4 is OFF & switch Q_1 is ON. The phase winding magnetized by source, and current flows in V_{DC} - Phase L_1 - Q_1 - V_{DC} and produces magnetic flux, which is attract the rotor poles in to align position.

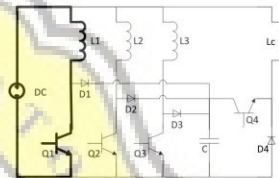


Fig. 3. Operation mode I

When switch Q_4 & Q_1 , condition is ON and when condition is OFF shown in Fig. 4, and Fig. 5. The current in the phase are flows thru phase of winding and the inductor L_C .

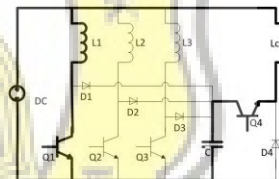


Fig. 4. Operation mode II

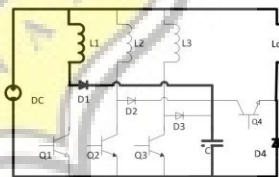


Fig. 5. Operation mode III

In Fig. 6, phase current in L_1 is start decreasing, because the demagnetization process. Q_1 is on and the energy in the winding is transfer into the capacitor dump, and the voltage level of the capacitor start increases to more than the V_{DC} source value. This additional of the voltage is used for the coil of the motor that would be use during the proses of the demagnetization in the winding that would be show in Fig. 7 below.

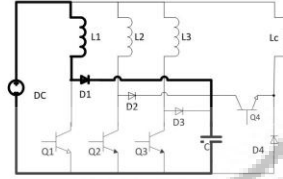


Fig. 6. Operation mode IV

In Fig. 7, the commutation of L_1 , by turning OFF switch in Q_1 . The Q_4 switch is turned to be ON, and transferring proses of the energy in dump capacitor into the voltage source. The additional negative voltage energy is for quick demagnetization in the stator winding. This very important features of conventional C-dump converter are full regenerative, freewheeling, simple control strategy & quick demagnetization proses.

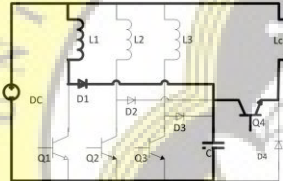


Fig. 7. Operation mode V

Complex chopper circuit control will be adds additional losses and costs due to more passive of components. Negative voltage depends on the capacitor value. Stable current commutation requires a larger V_0 which increasing the power device rating. Chopper circuit failure can cause uncontrolled capacitor charging. Search for new topologies of converter by reducing the switches but also have of advantages such as simplicity of control, regenerative, various operating speeds.

During mode I the equation of currents phase are given as the follows [1]:

$$i_{ph} = \frac{V_{dc}}{R_s} \left(1 - e^{-\frac{t}{\tau}} \right) + i_0(t) e^{-\frac{t}{\tau}} \quad (2)$$

Where,

i = Current RMS value in the phase winding

The equation for Voltage Dump Capacitor is:

$$C_d = \frac{(1-d_t)}{f_c} \cdot \frac{I}{\Delta V_o} \quad (3)$$

III. RESULT AND DISCUSSION

PSIM software was used to simulate conventional C-dump converter. In the simulation results the source voltage used is 100v, the capacitor used is 500uF. The speed can be adjusted through reference values. The signal output of simulation can be seen in Fig. 8, Fig. 9, and Fig. 10. From Figure phase voltage below the negative signal is generated due to demagnetization of stator pole.

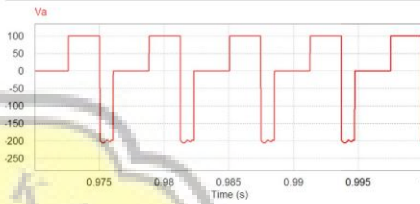


Fig. 8. PSIM Simulation of Voltage Phase

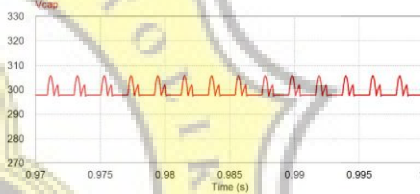


Fig. 9. PSIM Simulation of Capacitor Voltage

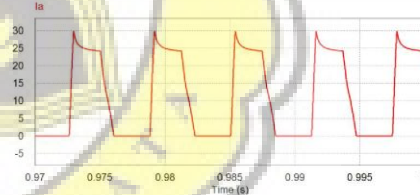


Fig. 10. PSIM Simulation of Current Phase

The 8/6 Switched Reluctance Motor that use conventional C-dump converter. The parameter of the motor that required for this simulation are already calculated using the equation that the parameter that using input source voltage 10 volt and the capacitor value is 470uF. The Voltage parameter values read and compare using the voltage sensor LEM LV25-P that installed parallel in capacitor, with dsPIC30F4012 for controller. The switch for this converter is IRFP250N. The

drive this converter use is TLP250 and buffer 74HC541N, and for rotor position sensor for this motor is hall effect.



Fig. 1. Switched Reluctance Motor and Converter

In Fig. 12, show I_a (Red), I_b (Purple), I_c (Blue) of current that flow from each phase, Fig. 13 show V_a (Red), V_b (Purple), V_c (Blue) Voltage of each phase, Fig. 14 show source voltage and capacitor. In this experiment capacitor voltage can be reach 14.6 Volt and the speed is reach 1792 RPM.

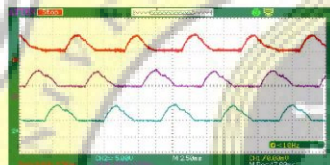


Fig. 11. Experimental result of current phase

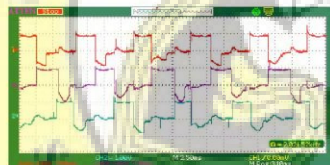


Fig. 12. Experimental result of voltage phase (voltage scale 10x)

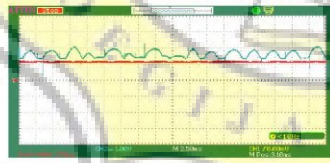


Fig. 13. Experimental result of capacitor and source voltage (voltage scale 10x)

In Fig. 15, show I_a (Red), I_b (Purple), I_c (Blue) of current that flow from each phase, Fig. 16 show V_a (Red), V_b (Purple),

V_c (Blue) Voltage of each phase, Fig. 17 show source voltage and capacitor. In this experiment capacitor voltage can be reaches a maximum value of 28 Volt and the maximum speed is reach 1937 RPM.

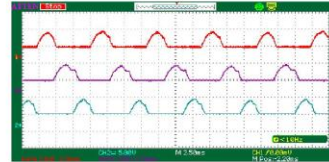


Fig. 14. Experimental result of current phase

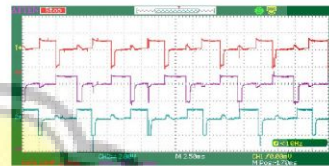


Fig. 15. Experimental result of voltage phase (voltage scale 10x)

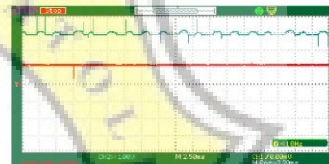


Fig. 16. Experimental result of capacitor and source voltage (voltage scale 10x)

Parameter Q4 ON (Freewheeling) In Fig. 18, show I_a (Red), I_b (Purple), I_c (Blue) of current that flow from each phase, Fig. 19 show V_a (Red), V_b (Purple), V_c (Blue) Voltage of each phase, Fig. 20 show source voltage and capacitor voltage. In this experiment capacitor voltage can be reach only 12 Volt so that the demagnetization value is not maximal and produces a negative torque which makes the speed result is only reach 1727 RPM.

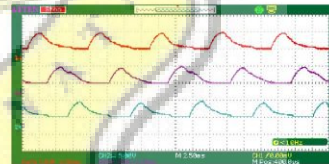


Fig. 17. Experimental result of current phase

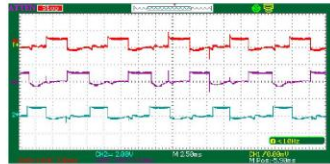


Fig. 18. Experimental result of voltage phase (voltage scale 10x)

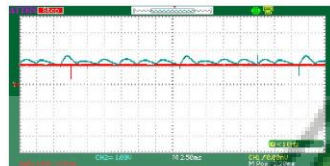


Fig. 19. Experimental result of capacitor and source voltage (voltage scale 10x)


IV. CONCLUSION

This converter derived from conventional C-dump converters are introduced in this paper. This converter can produce high speed, low voltage, and low current, and simple controls. The experimental results show good performance compared to the results of this simulation. This converter is interesting because the use of capacitors is set at a certain position and a 470 μF capacitor is used for this drive circuit to reach a fast discharge. The voltage rate in capacitor is 3 times the source value. When the voltage under the simulation the result speed are not in maximum value, this happen because the negative voltage also can have a full regenerative ability to perform a demagnetization system to minimize negative torque. The voltage rating of the device used in the converter is lowered to the input voltage, which is good for significant in low voltage power supply applications.

REFERENCES

- [1] Jibin Zou, Kai Liu, Jianhui Hu, Junlong Li, "A Modified C-Dump Converter for BLDC Machine used in Flywheel Energy Storage System", IEEE Transaction on Magnetics, Vol. 47, no. 10, pp. 4175-4178, October 2011.
- [2] F. Soares and P. I. Costa Branco, "Simulation of a 6/4 switched reluctance motor based on Matlab/Simulink environment," Aerospace and Electronic Systems, IEEE Transactions on, vol. 37, pp. 989-1009, 2001.
- [3] J. I. E. Miller, Electronic Control of Switched Reluctance Machines, Oxford, UK: Newnes Publishers, 2001.
- [4] R. Krishnan, "Switched Reluctance Motor Drives: Modeling, Simulation, Analysis, Design and Application" CRC press: 2001.
- [5] Y.Yoon; S. Song; T. Lee; C. Won; Y. Kim, "High Performance Switched Reluctance Motor Drive For Automobiles Using C-dump Converters", IEEE conference, Industrial Electronics, 2004 IEEE International Symposium, Paris, May 2004.
- [6] H. Bagherian, M. Asgar, E. Afjei, "A new Converter for Bifilar Winding Switched Reluctance Motor", 2nd Power Electronics, Drive Systems and Technologies Conference, IEEE Conference 2011, pp. 467-472.
- [7] F. Faradjizadeh, M. R. Tavakoli, M. Salehnia and E. Afjei, "C-Dump Converter for Switched Reluctance Generator" IEEE Conference, Drive System and Technology, February 2014.

- [8] M.Anand, V. Arunkumar, Dr. K. Krishnamurthy, Dr. B. Meenakshipriya, "Analysis and Modelling of Different Types of Converter in Switched Reluctance Motor for Reducing the Torque Ripple", 978- 1-4799-68 18- 3115@2 015 IEEE

3,948 

FORMULIR SCAN ANTI PLAGIARISME

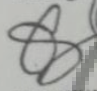
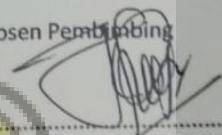
Nama : Kho Lukas Budi Setiawan

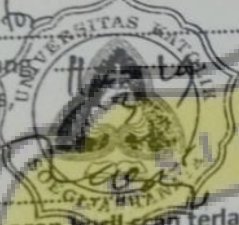
Alamat email : Kho. Lukas. Budi.S @ Gmail . Com

Fak. / Prodi : Teknik / Elektro NIM: 14.01.0003

berupa(TESIS, TUGAS AKHIR, PROPOSAL, SKRIPSI, SUMMARY, LAPORAN KERJA PRAKTEK)

dengan judul : Analisa Tegangan Kapasitor Pada Kaverter
C-Dump untuk Penggerak Switched Reluctance
Motor

Semarang  Yang Meyerahkan Dosen Pembimbing 

Petugas  untuk Yang bersangkutan *

NB. Laporan hasil scan terlampir 